scientific reports

Check for updates

OPEN

Carnosol exerts anti-inflammatory effects in pulpitis by inhibiting the RAGE/NF-κB signalling pathway

Xinpai Liu[1,4], Chunhui Zhao[1,4], Xirun Zong[1], Wenjing Fang[1], Jing Zhang[1,2]✉, Wei He[1,3]✉ & Wuli Li[1]✉

Effective pulpal inflammation control remains a global challenge. This study evaluated the protective efficacy of carnosol (CA) and its underlying mechanism both in vivo and in vitro. Human dental pulp cells (hDPCs) were isolated from third molars or orthodontically healthy teeth and treated for 6 h with 1 μg/mL lipopolysaccharide (LPS) alone or in combination with CA. Levels of receptor for advanced glycation end products (RAGE), interleukin (IL)-1β, IL-6, and tumour necrosis factor -α, and nuclear factor kappa B (NF-κB) activity, were examined. Sprague-Dawley rats were divided into: drilled (pulp exposure), CA-treated, DMSO-treated, and intact controls CA treatment at 2.5, 5, and 10 μM markedly suppressed pro-inflammatory cytokine expression in LPS-treated hDPCs in a concentration-dependent manner. CA treatment suppressed LPS-induced RAGE expression, reduced NF-κB phosphorylation, and blocked nuclear translocation of the NF-κB p65 subunit in hDPCs. RAGE silencing inhibited the NF-κB signalling pathway, leading to reduced inflammatory cytokine expression, and enhanced anti-inflammatory capacity of CA in vitro. CA treatment modulated RAGE mRNA expression without affecting the stability of the RAGE protein. In rats, CA administration to inflamed dental pulp reduced pulpal inflammation. CA alleviates pulpal inflammation through the RAGE/NF-κB pathway, which indicates its potential as a therapeutic option for managing pulpitis.

Keywords Pulpitis, Carnosol, AGE-RAGE signalling pathway, Inflammatory cytokine, NF-κB signalling pathway

Abbreviations

CA	carnosol
CCK-8	cell counting kit-8
CHX	cycloheximide
DMSO	dimethylsulfoxide
GO	Gene Ontology
hDPCs	human dental pulp cells
HE	haematoxylin and eosin
HMGB1	high-mobility group box 1
KEGG	Kyoto Encyclopedia of Genes and Genome
LPS	lipopolysaccharide
NF-κB	nuclear factor kappa B
PBS	phosphate-buffered saline
RAGE	receptor for advanced glycation end products
si-RAGE	RAGE small interfering RNA
si-NC	control siRNA
TBST	Tris-buffered saline with Tween 20

Pulpitis is a common dental inflammatory condition characterised by severe, persistent tooth pain. If left untreated, it can lead to pulpal necrosis, periapical lesions, tooth loss, abscess formation, or systemic infections,

[1]College & Hospital of Stomatology, Key Lab. of Oral Diseases Research of Anhui Province, Anhui Medical University, 69# Mei Shan Road, Hefei 230032, Anhui, China. [2]Faculty of Dentistry, The University of Hong Kong, Pok Fu Lam 999077, Hong Kong, China. [3]School of Basic Medical Sciences, Anhui Medical University, 81#Mei Shan Road, Hefei 230032, Anhui, China. [4]Xinpai Liu and Chunhui Zhao contributed equally to this work. ✉email: jing817@hku.hk; weihe@ahmu.edu.cn; 2008520001@ahmu.edu.cn

which may result in fever and increased discomfort[1–3]. These complications pose substantial health risks to patients. The standard treatment for pulpitis is root canal therapy, wherein the entire pulp is removed. However, pulp vitality is essential for preserving the normal metabolic and physiological functions of the tooth[4]. Therefore, preserving live pulp in cases of pulpitis presents a major challenge for endodontists worldwide. Effective control of pulpal inflammation is vital in determining the fate of the pulp[5–8]. Moderate inflammation helps eliminate harmful agents and promotes self-repair, thus preserving its vitality. In contrast, excessive inflammation can lead to pulpal necrosis, requiring pulp removal[9]. A promising treatment approach is the development of novel drugs that can effectively preserve the living pulp and manage pulpal inflammation.

Carnosol (CA), a phenolic diterpenoid derived from rosemary and sage plants[10], was first chemically characterised by Brieskorn et al.[11]. Studies have highlighted the antioxidant, anti-inflammatory, antimicrobial, immune-modulatory, and anticancer properties of CA[10,12]. CA has shown potential in treating various inflammatory conditions, including dermatitis[13], rheumatoid arthritis[14], and autoimmune encephalomyelitis[15]. However, its application in treating oral inflammatory diseases remains limited. While there is substantial evidence supporting the benefits of sage and rosemary for oral health[16–18], further research is needed on their active compounds in this context. In European herbal medicine, sage tea is commonly recommended for alleviating sore throats, oral inflammation, and gingivitis[19], and sage has demonstrated antibacterial properties against oral pathogens[20]. Rodrigues et al. also reported that sage leaf compounds, including sageol and ursolic acid/oleanolic acid, reduce pain and improve abnormal pain perception in murine models[21]. Additionally, a randomised, controlled, double-blind study found rosemary toothpaste to be effective in treating gingivitis[22]. Therefore, CA may also be effective in reducing pulpal inflammation.

A pattern recognition receptor of the immunoglobulin (Ig) receptor superfamily, receptor for advanced glycation end products (RAGE), interacts with various ligands, including high-mobility group box (HMGB)-1 and advanced glycation end products[23,24]. RAGE expression is low under normal physiological conditions but considerably increases during chronic inflammation due to the accumulation of various RAGE ligands[25]. In inflammatory states, the RAGE-ligand axis plays a central role in conditions such as diabetic complications[26], cardiovascular diseases[27], neurodegenerative disorders[28], cancer[29], and various inflammatory conditions. The RAGE-ligand signalling pathway is also a crucial mediator of nuclear factor kappa B (NF-κB) activation, oxidative stress, endothelial dysfunction, and pro-inflammatory cytokine expression[30]. Furthermore, previous studies have demonstrated that elevated RAGE expression in inflamed human pulpal tissues is strongly associated with the progression of pulpitis[31,32]. However, the specific role of RAGE in this pathological process remains to be further elucidated.

The potential of CA in alleviating pulpal inflammation was explored in this study. For this purpose, we first investigated the influence of CA treatment on cell proliferation and pro-inflammatory mediator expression in lipopolysaccharide (LPS)-stimulated human dental pulp cells (hDPCs) for in vitro analysis and a rat pulpitis model for in vivo analysis. Thereafter, the anti-inflammatory mechanism of CA via the RAGE and NF-κB signalling pathways was explored. Finally, the in vitro findings were validated through histological examination, haematoxylin and eosin (HE) staining, and immunohistochemistry in a rat pulpitis model.

Results

CA demonstrates no effects on hDPC viability with or without LPS stimulation

Immunohistochemical staining of isolated hDPCs showed strong positive reactivity for vimentin (Fig. 1A) and negative reactivity for keratin (Fig. 1B), consistent with typical hDPC characteristics.

The CCK-8 assay results, which were used to assess CA cytotoxicity on hDPCs, revealed no significant cytotoxicity at 2.5, 5, and 10 μM CA in comparison with 0 μM CA in the presence or absence of LPS (Fig. 1C, $P > 0.05$). Therefore, CA concentrations of 2.5, 5, and 10 μM were considered for further evaluation.

CA inhibits IL-6, IL-1β, and TNF-α expression in LPS-induced hDPCs

Scatterplots for RNA sequencing data revealed that IL-6, TNF-α, and IL-1β expression was downregulated in the LPS + CA group compared with that in the LPS group (Fig. 2A). The qRT-PCR analysis showed that CA + LPS treatment led to a significant dose-dependent reduction in the *IL-6*, *IL-1β*, and *TNF-α* mRNA levels in hDPCs (Fig. 2B–D). WB and ELISA confirmed that CA treatment markedly decreased the IL-6, IL-1β, and TNF-α protein levels in hDPCs. At 10 μM, CA treatment reduced inflammatory cytokine levels to nearly those observed in the control samples (Fig. 2E–H). Additionally, CA exhibited a weak inhibitory effect on inflammatory cytokine expression in the absence of LPS (Supplementary Fig. 1).

CA inhibits LPS-induced RAGE production, NF-κB phosphorylation, and NF-κB p65 nuclear translocation in hDPCs

The Gene Ontology (GO) and Kyoto Encyclopedia of Genes and Genomes (KEGG) enrichment analyses of RNA sequencing data revealed that CA might exert its anti-inflammatory effects through the AGE-RAGE and NF-κB signalling pathways (Fig. 3A and B). qRT-PCR revealed a significant dose-dependent decrease in *RAGE* mRNA expression in the hDPCs pre-treated with CA before LPS exposure in comparison with that in the hDPCs treated with LPS alone (Fig. 3C). The WB analysis confirmed this reduction at the protein level, with 10 μM CA reducing RAGE expression to levels similar to those in the control samples (Fig. 3D).

Further investigation into NF-κB revealed that CA treatment significantly reduced NF-κB phosphorylation and p-p65 expression in LPS-stimulated hDPCs, with CA (5 μM) nearly inhibiting NF-κB p65 phosphorylation (Fig. 3E). Immunofluorescence staining demonstrated that CA effectively reduced p65 nuclear translocation induced by LPS, demonstrating its effect on the NF-κB signalling pathway (Fig. 3F, G).

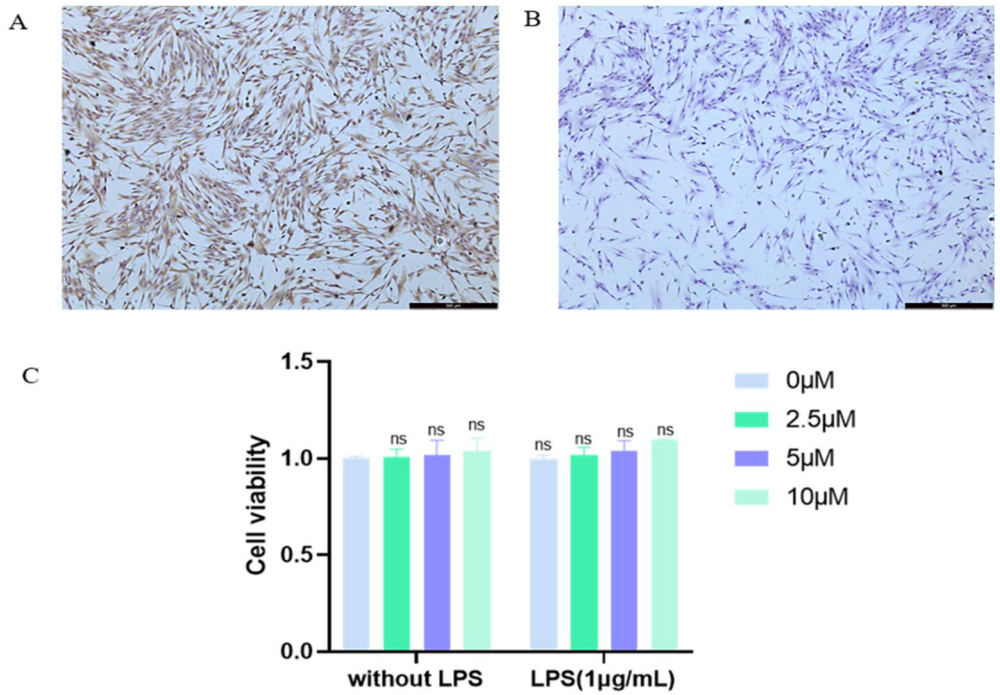

Fig. 1. hDPCs identification and assessment of the effect of CA on hDPC viability. (**A**) Positive vimentin staining (50× magnification); (**B**) Negative keratin staining (50× magnification). Scale bar, 500 μm. (**C**) Assessment of hDPC viability following treatment with 0, 2.5, 5, and 10 μM CA in the presence or absence of LPS. Data are presented as mean ± standard deviation of values from three independent experiments. Data were analyzed by two-way analysis of variance (ANOVA) followed by Sidak's multiple comparisons test. ns: $P > 0.05$.

CA-mediated pulpal inflammation resolution is dependent on RAGE in hDPCs

To investigate whether CA-mediated pulpal inflammation resolution is dependent on RAGE, we co-treated hDPCs with LPS and siRNA-RAGE. The WB analysis revealed that RAGE protein expression in the si-RAGE + LPS group was significantly lower than in the LPS-only group, confirming effective RAGE knockdown (Fig. 4A). CA pre-treatment did not affect this knockdown, indicating that RAGE expression was substantially suppressed by siRNA-RAGE.

Additionally, the qRT-PCR analysis showed that the si-RAGE + LPS group had significantly lower IL-6, IL-1β, and TNF-α mRNA levels than the LPS group, with levels approaching those of the control group (Fig. 4B–D). However, RAGE silencing abolished the modulatory effects of CA on IL-6, IL-1β, and TNF-α levels in hDPCs. This finding suggests that RAGE is crucial for the regulation of inflammation in pulpitis.

Immunofluorescence staining showed that CA did not have a significant role on the nuclear translocation of p65 from cytoplasm in si-RAGE-transfected hDPCs with LPS stimulation, although preventing p65 translocation was observed in si-RAGE-transfected hDPCs and CA-treated hDPCs with LPS stimulation (Fig. 4E, F). This finding indicates the crucial role of RAGE in CA-mediated resolution of pulpal inflammation in hDPCs.

CA inhibits the transcription of RAGE

We sought to elucidate the regulatory mechanism by which CA reduces RAGE protein expression. At 6 h post-treatment, the influence of CA on RAGE mRNA expression in hDPCs (in the absence of LPS stimulation) was assessed by qRT-PCR, while RAGE protein levels were analyzed at 24 h by WB. We found that CA treatment induced a significant, dose-dependent inhibition of both RAGE mRNA (at 6 h) and protein synthesis (at 24 h) ($P < 0.05$; Fig. 5A and B). Furthermore, we treated hDPCs with cycloheximide (CHX), a eukaryotic protein synthesis inhibitor that blocks translational elongation, either alone or in combination with CA. The results demonstrated that the degradation of RAGE protein over time did not differ significantly between the CHX-treated group and the CHX + CA co-treatment group ($P > 0.05$; Fig. 5C, D). These data suggest that CA-mediated reduction of RAGE occurs primarily at the transcriptional level rather than through post-translational regulation of protein stability in hDPCs.

CA alleviates inflammatory responses in the rat model of pulpitis

A pulpitis model of Sprague–Dawley rats was developed to evaluate the influence of CA treatment on inflamed pulp tissues. Inflammatory cell infiltration was assessed in each experimental group using HE staining. The results showed that rats subjected to drilled pulp exposure followed by CA (50 μM, 3 μL) treatment exhibited reduced neutrophil infiltration, more organised odontoblast arrangement, and minimal vasodilation compared with rats receiving drilled treatment alone (Fig. 6).

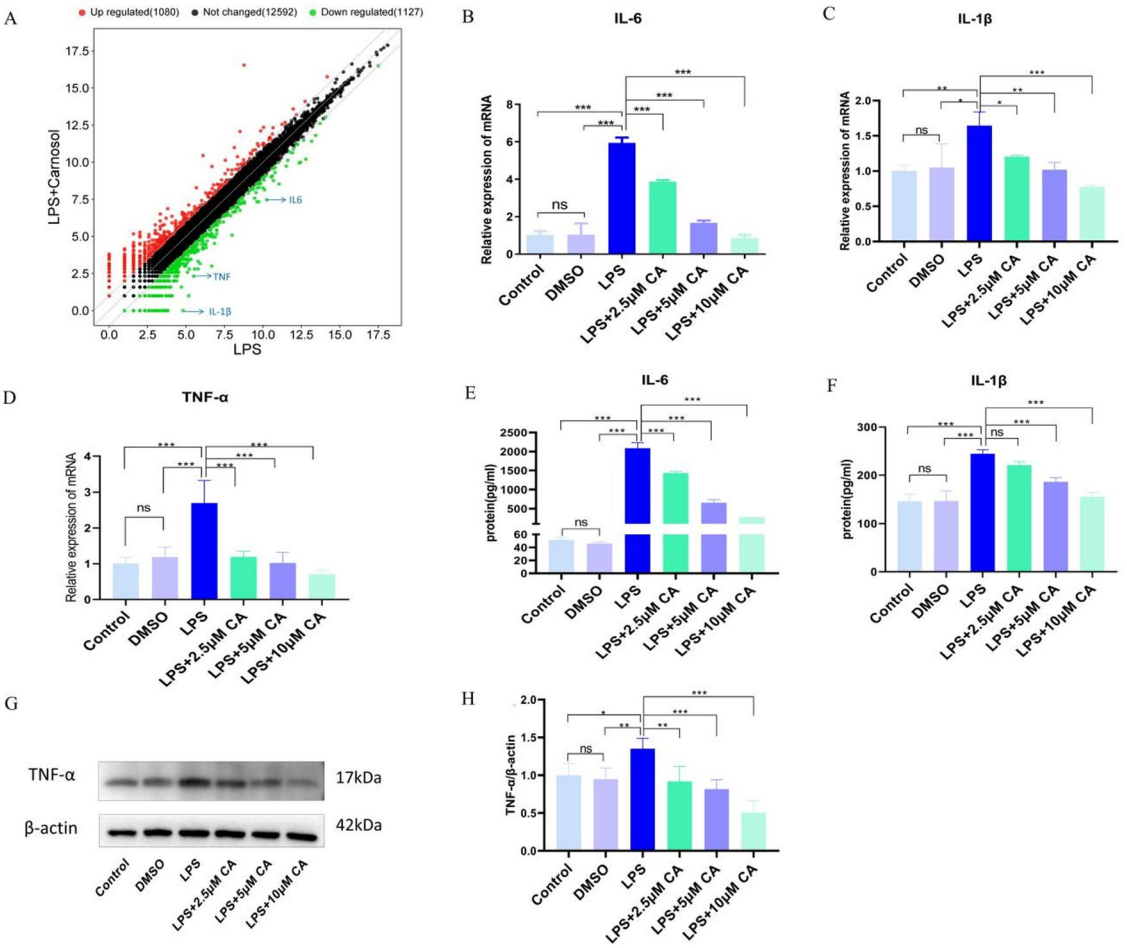

Fig. 2. CA attenuates LPS-induced inflammation in hDPCs. (**A**) Scatterplots of differentially expressed genes. (**B**–**D**) mRNA expression levels of IL-6, IL-1β, and TNF-α. (**E**, **F**) Protein expression levels of IL-6 and IL-1β assessed using ELISA. (**G**) Protein expression levels of TNF-α assessed using WB. (**H**) The quantitative expression of TNF-α detected by densitometry. Data are presented as mean ± standard deviation of values from three independent experiments. Data were analyzed by one-way ANOVA (B, C, D, E, F, H) followed by Tukey's multiple comparisons test. $^{*}P<0.05$; $^{**}P<0.01$; $^{***}P<0.001$.

CA reduces RAGE, p-p65, and IL-1β expression in the rat model of pulpitis

The immunohistochemical analysis of the RAGE/NF-κB signalling pathway in the drilled group revealed a higher number of RAGE-positive (Fig. 7A, D), p-p65-positive (Fig. 7B, E), and IL-1β-positive (Fig. 7C, F) cells. This group displayed intense brownish-yellow staining; in contrast, the drilled + CA-treated group showed markedly weaker staining and the control group exhibited minimal staining of pulp cells. The quantitative results showed the level of RAGE, p-p65 and IL-1β was reduced effectively in the drilled + CA group compared with that in the drilled + DMSO group (Fig. 7).

Discussion

Extensive clinical and experimental studies over recent decades have aimed to develop new drugs or materials for effectively managing pulpal inflammation, facilitating minimally invasive treatments for pulpitis[1,8]. Unlike previous studies, which predominantly focused on synthetic compounds, the present investigation focused on natural herbal medications with anti-inflammatory properties, which offer potential benefits with fewer adverse effects[18,33,34]. The anti-inflammatory properties of CA have been explored across various inflammatory conditions, along with its ability to inhibit oral bacterial growth[35]. We investigated the potential of CA to mitigate pulpitis in this study and examined its underlying mechanism. This is the first study to show CA-mediated anti-inflammatory effects on pulpitis through inhibition of the RAGE/NF-κB pathway.

Our study demonstrated that CA reduces inflammatory mediator secretion by inhibiting NF-κB signalling in hDPCs treated with LPS, aligning with previous study findings[36–39]. CA suppresses NF-κB activation under different inflammatory conditions[36–38], including attenuating inducible nitric oxide synthase, IL-1α, IL-6, CXCL10, and CCL5 expression. It also inhibits nuclear translocation of NF-κB p65, induced by IL-1β, in chondrocytes[37]. Moreover, CA reduces serum IL-6 level, neutrophil infiltration, and hepatic intracellular adhesion molecule-1 expression, ultimately attenuating intestinal ischemia–reperfusion-induced liver injury

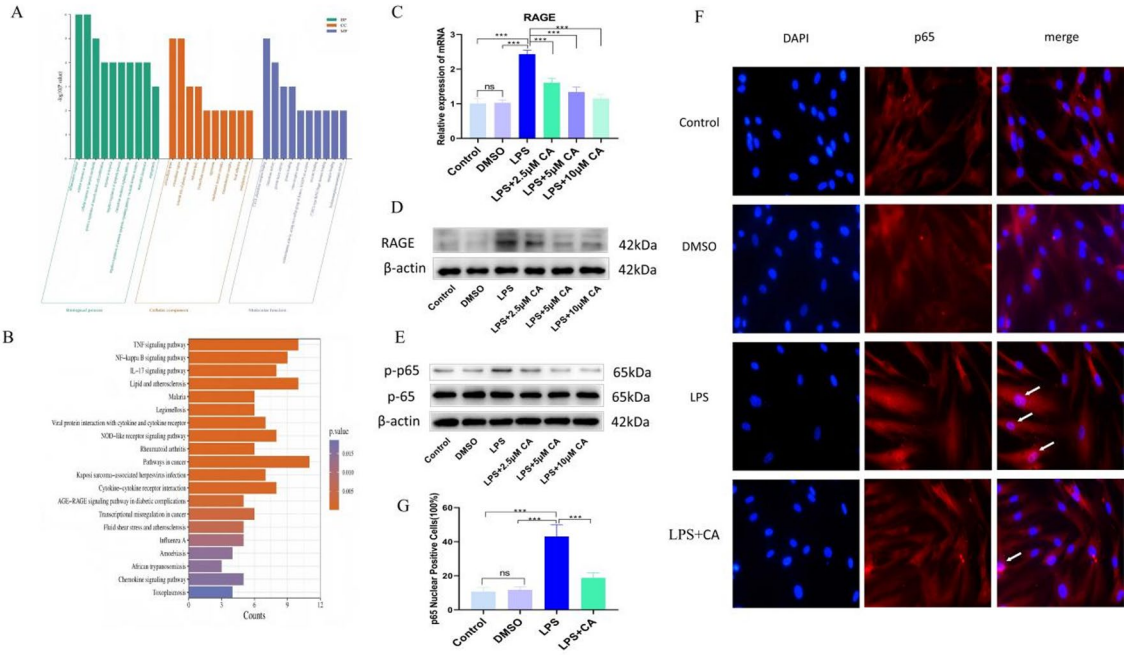

Fig. 3. Effect of CA on the RAGE/NF-κB pathway in LPS-stimulated human dental pulp cells (hDPCs). (**A**) GO enrichment analysis of differentially expressed genes. (**B**) KEGG analysis of differentially expressed genes. (**C**) Relative expression of RAGE mRNA following CA pre-treatment of hDPCs and stimulation with LPS. (**D**) Protein expression of RAGE in hDPCs pre-treated with CA and stimulated with LPS, as detected through western blotting (WB). (**E**) Protein expression of p65 and phosphorylated p65 (p-p65) assessed via WB. (**F**) Cytoplasmic and nuclear localisation of p65 (400× magnification). (**G**) The quantitative expression of p65 was measured by counting the quantity of positive cells. Arrows indicate p65 translocation into the nucleus. Data are presented as mean ± standard deviation of values from three independent experiments. Data were analyzed by one-way ANOVA (C, G) followed by Tukey's multiple comparisons test. $^{***}P < 0.001$.

by suppressing NF-κB p65 nuclear translocation[39]. Additionally, CA has been shown to reduce inflammation in microglia; decrease IL-1β, TNF-α, and IL-6 levels[40]; and inhibit inflammatory cell infiltration and cytokine expression in colonic tissue[39], suggesting its potential for treating rheumatoid arthritis[14]. In mice, it also alleviates epidermal thickening, UVB-induced erythema, and inflammatory responses[13]. Furthermore, CA prevents activation of the NLRP3 inflammasome by targeting heat shock protein 90, offering therapeutic potential in inflammasome-mediated inflammatory conditions[41]. Our in vitro and in vivo analyses further support the anti-inflammatory effects of CA in alleviating pulpal inflammation. However, the precise mechanism through which CA regulates pulpitis requires further investigation.

The RNA sequencing and KEGG analyses suggest the involvement of the AGE-RAGE and NF-κB signalling pathways, indicating their potential roles in the CA-mediated anti-pulpitis effect. This study showed that CA significantly inhibited RAGE production in LPS-stimulated hDPCs, and si-RAGE treatment suppressed IL-6, IL-1β, and TNF-α expression. This finding underscores the crucial role of RAGE in pulpitis development, aligning with previous reports[31,32]. Zhang et al. reported increased RAGE expression in clinically inflamed pulp compared with that in healthy pulp, implicating RAGE and HMGB1 in both dental pulp inflammation and stem cell recruitment, potentially promoting pulp repair and regeneration[32]. Tancharoen et al. demonstrated the crucial function of RAGE in mediating the immune response of pulp to oral bacterial infections[31]. Upregulated RAGE signalling and its ligand expression have been reported in rheumatoid arthritis[42], inflammatory bowel disease[43], and other pathological states[30,44,45]. Animal models of these diseases suggest that targeting RAGE therapeutically inhibits chronic inflammation[13,14,46–48]. Our results demonstrated that CA targets RAGE to modulate pro-inflammatory cytokine expression in pulpitis, contributing to its anti-inflammatory effects.

To confirm that the CA-mediated suppression of RAGE was not due to changes in protein stability, we assessed RAGE protein expression following treatment with CHX, a cytoplasmic protein synthesis inhibitor, with or without CA. The results indicated that CA did not affect RAGE protein stability in hDPCs. Gene regulation involves complex mechanisms, at the transcriptional, translational, and post-translational levels[49]. Our findings suggest that CA regulates RAGE expression primarily through transcriptional mechanisms rather than post-translational mechanisms.

Our results suggest that RAGE is a crucial mediator of NF-κB activation, promoting pro-inflammatory cytokine expression in pulpitis. This is in accordance with the findings of prior studies indicating that RAGE activation triggers NF-κB signalling, resulting in increased cytokine expression and exacerbating inflammation[30,50]. We observed that LPS treatment upregulated inflammatory cytokine expression and induced

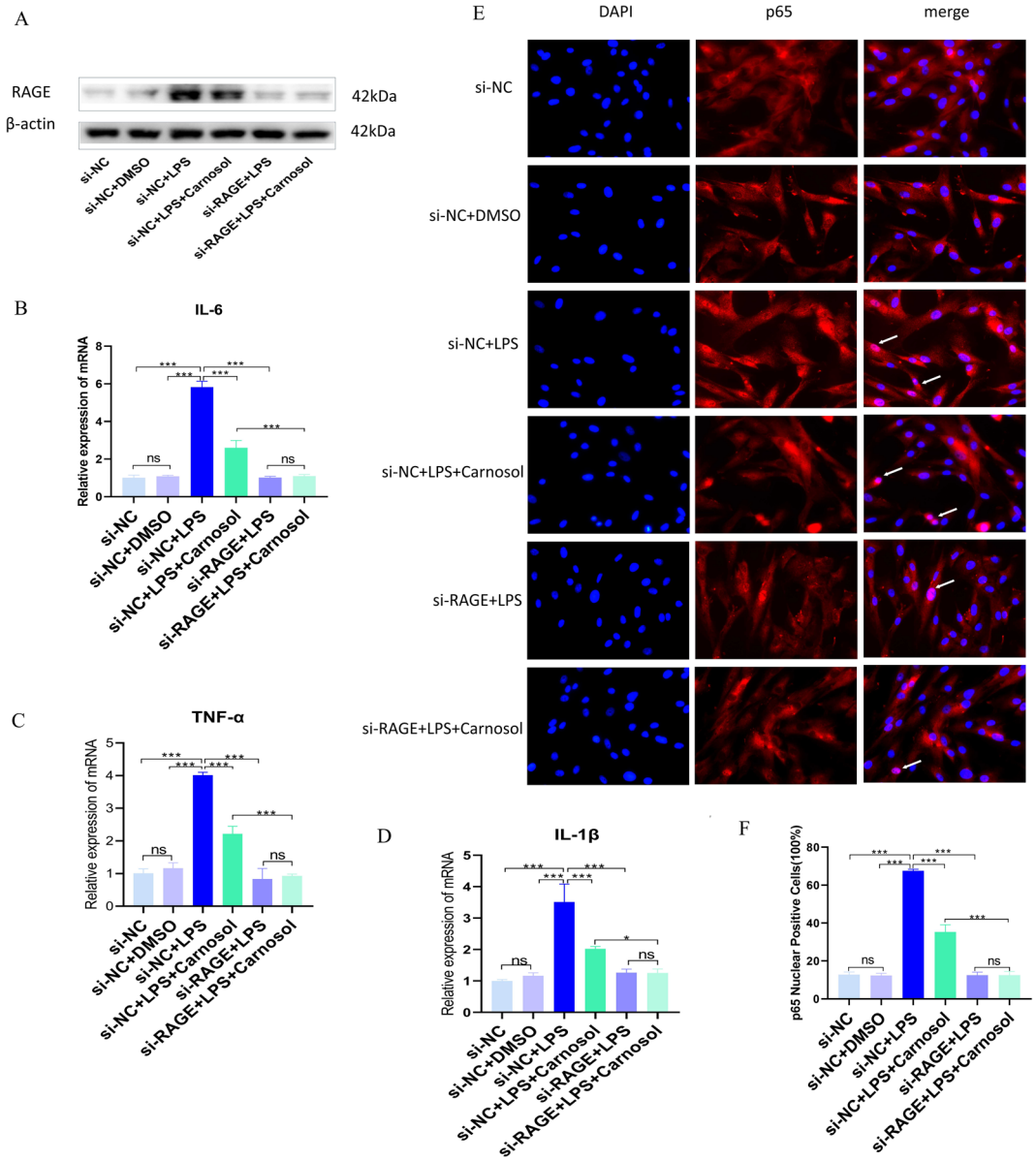

Fig. 4. RAGE is involved in pulpal inflammation resolution induced by CA. (**A**) Efficiency of RAGE knockdown. (**B**) IL-6 mRNA expression following RAGE knockdown with or without CA in LPS-treated hDPCs. (**C**) TNF-α mRNA expression following RAGE knockdown with or without CA in LPS-treated hDPCs. (**D**) IL-1β mRNA expression following RAGE knockdown with or without CA on LPS-treated hDPCs. (**E**) Effect of RAGE knockdown in LPS-treated hDPCs with or without CA on the NF-κB activity (400× magnification). Arrows indicate p65 translocation into the nucleus. (**F**) The quantitative expression of p65 was measured by counting the quantity of positive cells. Data are presented as mean ± standard deviation of values from three independent experiments. Data were analyzed by one-way ANOVA (**B**, **C**, **D**, **F**) followed by Tukey's multiple comparisons test. $^{*}P < 0.05$; $^{***}P < 0.001$.

p65 nuclear translocation in hDPCs; in contrast, CA treatment significantly decreased the expression of IL-6, IL-1β, and TNF-α following LPS stimulation. We also observed reduced p65 translocation to the nucleus after CA treatment. Inhibiting RAGE expression induced a similar inhibitory effect; however, the reduction was more pronounced. These observations indicate that the anti-inflammatory effects of CA may be mediated by impeding RAGE/NF-κB signalling pathway activation. The animal experiment results corroborated these in vitro findings, as CA administration reduced RAGE, p65, and IL-1β expression in inflamed dental pulp in rats, indicating reduced inflammation. Collectively, the findings of this study highlight the potential therapeutic value of CA in the clinical management of pulpitis.

However, this study has several limitations. First, we did not analyze odontoblast cell death, a critical factor in pulp inflammatory processes. As our experiments focused on verifying RAGE signaling, odontoblast cell death was not evaluated. This gap limits the comprehensiveness of our findings, as we could not link changes in

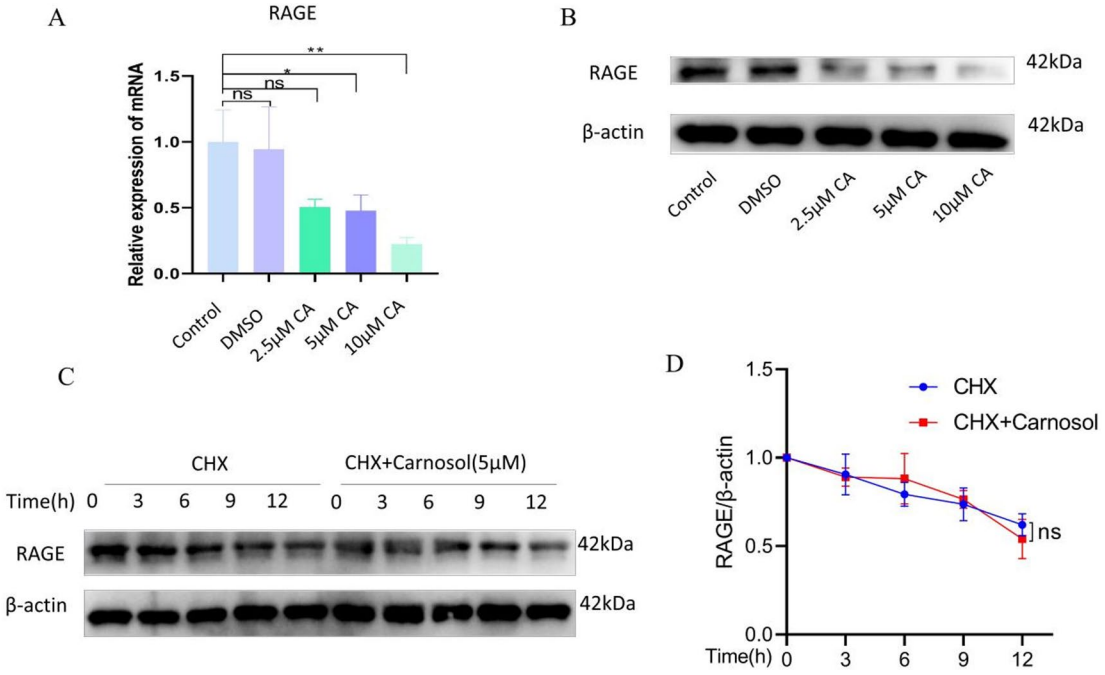

Fig. 5. Effect of CA on the transcription of RAGE. (**A**) qRT-PCR analysis of CA's effect on RAGE mRNA synthesis. (**B**) WB analysis of CA's effect on RAGE protein expression. (**C**) WB analysis of CA's effect on RAGE protein stability. (**D**) RAGE protein expression levels over time. Data are presented as mean ± standard deviation of values from three independent experiments. Data were analyzed by one-way ANOVA (A) followed by Tukey's multiple comparisons test or two-way ANOVA (D) followed by Sidak's multiple comparisons test. $^{*}P < 0.05$; $^{**}P < 0.01$.

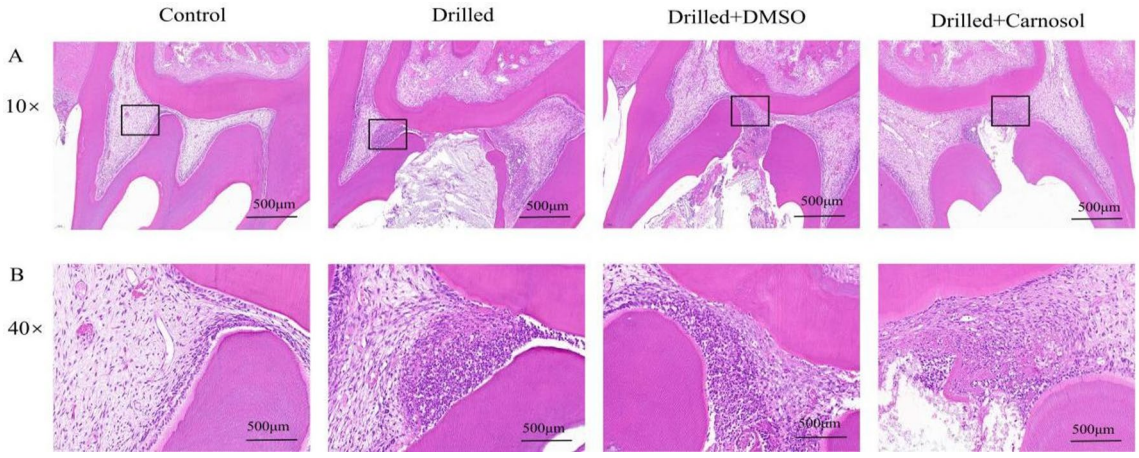

Fig. 6. Representative H&E staining illustrating histopathological changes in dental pulp inflammation in rats treated with CA. (**A**) Low magnification micrograph of dental pulp showing inflammatory changes. Black box: lesion site. (**B**) High magnification micrograph showing detailed histopathological alterations in the dental pulp. The sample size for each group was $n = 6$.

RAGE expression to pulp tissue damage or clarify RAGE's role in regulating odontoblast survival. Future studies should quantify odontoblast cell death (e.g., via TUNEL staining) and integrate these data with assessments of RAGE signaling to improve understanding of pulpitis pathogenesis. Second, TNF-α and IL-6 are key mediators of pulpitis progression, and the lack of their in vivo detection is another limitation. Investigating TNF-α/IL-6 expression in vivo would therefore enhance our understanding of the anti-inflammatory role of CA in pulpitis pathogenesis.

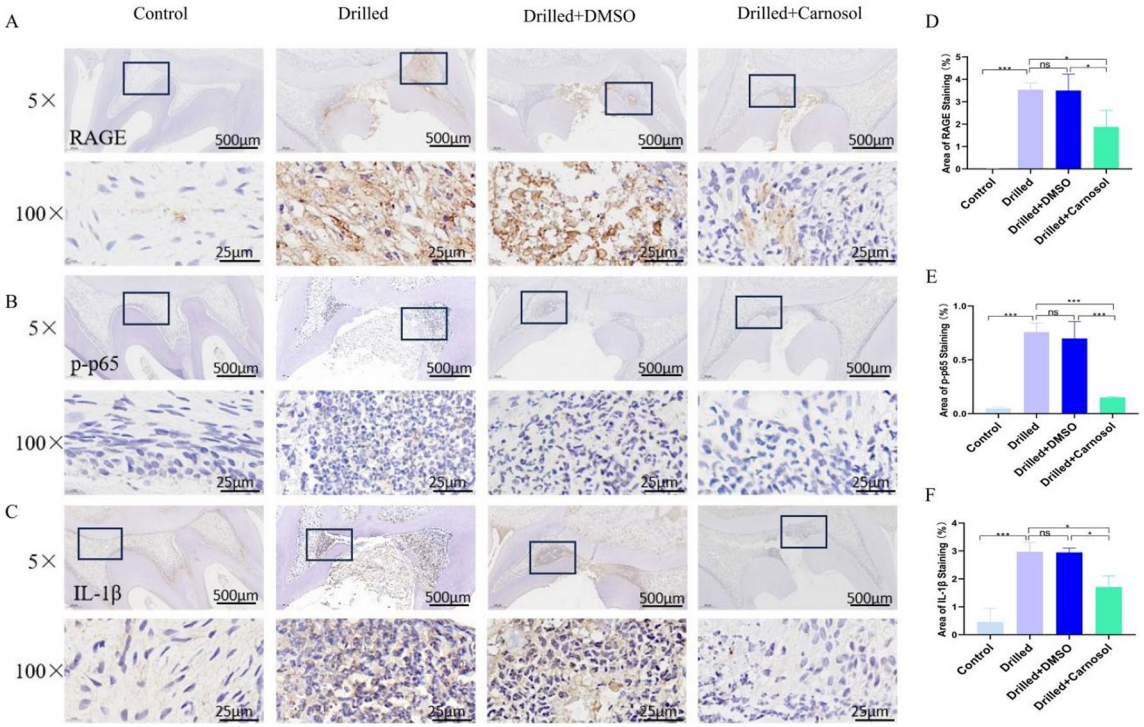

Fig. 7. Representative immunohistochemical staining of (**A**) RAGE; (**B**) p-p65; (**C**) IL-1β. Brown granules indicate positive expression of the respective proteins. For semi-quantitative analysis, the positive staining areas of (**D**) RAGE, (**E**) p-p65, and (**F**) IL-1β were quantified, and the results are presented as the percentage of positive staining area relative to the total tissue area. The sample size for each group was $n = 6$. All data are expressed as the mean ± standard deviation derived from three independent experiments. Statistical analyses were performed using one-way ANOVA followed by Tukey's multiple comparisons test. $^{*}P < 0.05$; $^{***}P < 0.001$.

Materials and methods

Cell isolation and culture

hDPCs, isolated from third molars or orthodontically healthy teeth requiring extraction from patients aged 18–30 years, were obtained from the Affiliated Stomatology Hospital of Anhui Medical University. The institutional medical ethics committee granted the ethical approval for this study (approval no. T2022023). After washing the extracted tooth samples using phosphate-buffered saline (PBS), the dental pulp was excised from the pulp cavity, sectioned, and enzymatically treated for 15 min with 3 mg/mL collagenase (Biofroxx, Germany). The tissue fragments were then centrifuged and evenly distributed on cell culture flasks. These flasks were incubated in a 5% CO_2 environment for 4–6 h at 37 °C until tissue adherence occurred. Subsequent cultures were maintained in a minimum essential medium (Gibco, USA) containing 0.1 mg/mL streptomycin, 100 U/mL penicillin, and 20% foetal bovine serum (Wisent, China). Further experiments were performed using cells from passages 4–6.

Cell counting Kit-8 (CCK-8) assay

hDPCs were seeded into 96-well plates (5×10^3 cells/well) and incubated overnight at 37 °C under 5% CO_2. Thereafter, the hDPCs were treated for 24 h with 2.5, 5, or 10 μM CA (Carnosol, with a purity of 99% was purchased from TargetMol, China. Its molecular formula is $C_{20}H_{26}O_4$ and molecular weight is 330.42. It was dissolved in DMSO to make a solution of 10 mM/ml and stored at -20 °C away from light), with or without 1 μg/mL LPS (Lipopolysaccharide, was derived from Escherichia coli O111: B4 and acquired from Sigma, America, lot no: L4391). Following treatment, the hDPCs were incubated for 2 h in a serum-free medium containing CCK-8 solution (Biosharp, China). A microplate reader (Tecan, China) was employed to measure the optical density of hDPCs at 450 nm.

RNA sequencing

For RNA sequencing, hDPCs were subjected to CA pre-treatment for 2 h, followed by LPS treatment for 6 h; subsequently, total RNA was extracted. Sample purification, library construction, and sequencing were outsourced to Personalbio Company in Shanghai, China. The Gene Ontology (GO) and Kyoto Encyclopedia of Genes and Genomes (KEGG) databases were used to conduct pathway and bioinformatic analyses.

Quantitative reverse transcription polymerase chain reaction (qRT-PCR)

TRIzol reagent (Invitrogen, USA) was used for total RNA extraction following the manufacturer's instructions. Next, the PrimeScript RT Reagent Kit (Takara, Japan) was employed to reverse transcribe 500 ng of the isolated RNA into complementary DNA, which was then subjected to qRT-PCR using the SYBR Green Master Mix Kit

(Yeasen, China) on the Stratagene Mx3000P qPCR system (Agilent Technologies, USA). The $2^{-\Delta\Delta Ct}$ method was employed to determine the relative target gene expression levels using β-actin as a reference. The primer sequences were as follows (5′ to 3′): interleukin (*IL*)-*6*, F: ACACAGACAGCCACTCACCT, R: CCAGTGCC TCTTTGCTGCTT; *IL-1β*, F: AACCTCTTCGAGGCACAAGG, R: AGCCATCATTTCACTGGCGA; tumour necrosis factor (*TNF*)-*α*, F: ATGGCGTGGAGCTGAGAGAT, R: TCTGGTAGGAGACGGCGATG; and *RAGE*, F: ACTACCGAGTCCGTGTCTACC, R: GGAACACCAGCCGTGAGTT. The β-actin primers were as follows: F: CTCCATCCTGGCCTCGCTGT, R: GCTGTCACCTTCACCGTTCC.

Western blot (WB) assay

To ensure protein stability, RIPA lysis buffer (Beyotime, China) containing protease inhibitor cocktail, 1 mM phenylmethanesulfonyl fluoride, and 1× phosphatase inhibitor cocktail was used for total protein extraction from hDPCs. The concentration of the extracted protein was measured using the BCA Protein Assay Kit (Beyotime, China). Thereafter, 20 μg of protein was loaded and separated via 12.5% sodium dodecyl sulphate–polyacrylamide gel electrophoresis (EpiZyme, China) and blotted onto 0.22-μm polyvinylidene difluoride membranes (Millipore, USA). These membranes were blocked for 2 h with 5% non-fat milk dissolved in Tris-buffered saline with Tween 20 (TBST) at room temperature (RT). After blocking, the membranes were cut to isolate the target strip and the internal reference strip, based on the molecular weight of the target protein and loading control, which could make the strips narrow. The isolated strips were then incubated with appropriate primary antibodies at 4 °C to determine the levels of the target protein and loading control. The primary antibodies included anti-TNF-α (1:1000, YT4689; Immunoway), anti-p65 (1:1000, A5075; Selleck), anti-p-p65 (1:1000, #3033; CST), anti-RAGE (1:500, WL01514; Wanleibio), and anti-β-actin (1:10000, EM21002; HUABIO) antibodies. Following this, the membranes were rinsed five times with TBST for 6 min each and treated for 45 min with horseradish peroxidase (HRP)-conjugated secondary antibodies (1:5000, ZB2305, ZB2301, ZSGB-Bio) on a rocking platform at RT. After another round of washing, the blots were visualised using a visualiser (Tanon, China) and an enhanced chemiluminescence detection kit (NCM Biotech, China). For normalisation, β-actin served as the loading control.

Enzyme-linked immunosorbent assay (ELISA)

hDPCs were subjected to CA pre-treatment for 2 h and LPS treatment for another 24 h. The culture medium was then harvested and subjected to centrifugation for 20 min at 1000 x *g* to remove debris. IL-1β and IL-6 levels in the resulting supernatants were quantified using IL-1β (Elabscience, China) and IL-6 (Dakewe, China) ELISA kits, following the manufacturers' instructions.

Detection of NF-κB activation and nuclear translocation

NF-κB activity was assessed using the NF-κB Activation, Nuclear Translocation Assay Kit (Beyotime, China). Briefly, hDPCs were pretreated by carnosol for 2 h and LPS for another 24 h, then fixed for 10 min and treated for 1 h with an immunostaining blocking solution at RT. Subsequently, the hDPCs were treated overnight with primary rabbit anti-NF-κB p65 antibodies at 4 °C and then incubated for 1 h with cyanine3-conjugated secondary antibodies at RT. The hDPCs were stained for 5 min with 4',6-diamidino-2-phenylindole for nuclear staining. The hDPCs were washed thrice for 5 min each after each treatment. A fluorescence microscope (Leica, Germany) was used to observe and image the hDPCs.

Cell transfection

hDPCs were initially seeded into six-well plates (1.5×10^5 cells/well). Transfection was initiated when the hDPCs attained approximately 50% density. The cells were transfected with 50 nmol/L control siRNA (si-NC) or RAGE small interfering RNA (si-RAGE) (General Biol, China) using Lipofectamine 2000 (Invitrogen, USA). After transfection for 6 h, the cells were cultured for 40 h in fresh complete medium. The transfected cells were then stimulated for 6–24 h with CA with or without LPS (Sigma, USA), after which they were harvested for analyses. The siRNA sequences were as follows (5′ to 3′): si-RAGE, F: GAAAGGAGACCAAGUCCAATT, R: UUGGAC UUGGUCUCCUUUCTT; si-NC, F: UUCUCCGAACGUGUCACGUTT, R: ACGUGACACGUUCGGAGAA TT.

Assessment of RAGE protein expression

hDPCs were pretreated with 25 nM cycloheximide (CHX) for 2 h, and then incubated for 3, 6, 9, and 12 h with or without 5 μM CA. Subsequently, cells were harvested, and RAGE protein expression was detected by WB.

Rat pulpitis model

All experimental animals were obtained from the Experimental Animal Center of Anhui Medical University. The ethical approval for the study was provided by the institutional medical ethics committee (approval no. LLSC20221248). Male Sprague–Dawley rats ($n = 24$; 6–8 weeks old) were segregated randomly into four groups. The rats were anaesthetised with 30 mg/kg pentobarbital sodium via intraperitoneal injection. The pulp cavity on one side of the upper first molars was accessed using #1/4 dental round diamond burs on high-speed handpieces and then enlarged to 1-mm depth using a #40 K file. The exposed pulp was left in contact with the oral environment for 12 h to induce pulpitis. After 12 h, the rats were anaesthetised again, and the pulp cavity was rinsed with 0.9% saline. The rats were then allocated into three treatment groups: the drilled group, the cavity was covered with a sterile gelatine sponge and sealed with glass ionomer cement; the drilled + CA group, 50 ng of CA solution was injected into the cavity; and the drilled + dimethyl sulfoxide (DMSO) group, the cavity was injected with 50 ng of DMSO solution. Both CA and DMSO solutions were diluted with PBS to ensure

that the DMSO content did not exceed 0.1%. The rats were euthanised after 3 d of treatment and samples were collected for further assessment.

Sample preparation and histological analysis

For histological staining, 6 rat dental pulp specimens were allocated to each group. These samples were fixed for 24 h in 4% paraformaldehyde and decalcified for approximately 6 weeks in 10% ethylenediaminetetraacetic acid solution (pH 7.2), which was changed on alternate days. The samples were paraffin-embedded, sectioned (5-μm), and mounted onto slides. Following deparaffinisation and rehydration, the sections were stained with HE to assess dental pulp inflammatory status. For immunohistochemical analysis, the deparaffinised sections were treated for antigen retrieval and then blocked for endogenous peroxidases (3% bovine serum albumin was used for blocking). Subsequently, the sections were treated overnight with the following primary antibodies at 4 °C: anti-p-p65 (1:50, AF5881; Affinity), anti-RAGE (1:1000, 16346-1-AP; Proteintech), and anti-IL-1β (1:200, AF5103; Affinity) antibodies. Thereafter, the sections were washed three times with PBS and incubated for 50 min with HRP-labelled secondary antibodies at RT. Colour development was conducted using a 3,3'-diaminobenzidine detection kit (Solarbio, China), and nuclear staining was performed with haematoxylin. The Panoramic MIDI scanner (3DHISTECH, Hungary) was used to capture images.

Statistical analysis

Statistical analyses were performed using GraphPad Prism 8. Data are presented as mean ± standard deviation. The significance of differences between groups was assessed using a one-way or two-way analysis of variance. Results with a P value of < 0.05 were considered statistically significant.

Conclusion

Our in vivo and in vitro findings demonstrate that CA suppresses inflammatory cytokine expression by targeting the RAGE/NF-κB signalling pathway. As a promising therapeutic agent derived from traditional herbal medicines, CA offers advantages, such as a low toxicity profile and cost-effectiveness. Therefore, the potential clinical application of CA in treating pulpitis warrants further investigation and increased attention in clinical research.

Data availability

Data will be made available by the corresponding author upon request.

Received: 2 July 2025; Accepted: 11 November 2025
Published online: 29 December 2025

References

1. Liu, X., Wang, C., Pang, L., Pan, L. & Zhang, Q. Combination of resolvin E1 and Lipoxin a4 promotes the resolution of pulpitis by inhibiting Nf-Kb activation through upregulating Sirtuin 7 in dental pulp fibroblasts. *Cell. Prolif.* **55**, e13227. (2022).
2. Nguyen, D. H. & Martin, J. T. Common dental infections in the primary care setting. *Am. Fam Physician.* **77**, 797–802 (2008).
3. Cardoso, A. S. & Mitchell, D. F. Progression of pulpitis to necrosis and periapical disease in deciduous and permanent teeth of monkeys. *J. Dent. Res.* **50**, 934–938 (1971).
4. Morotomi, T., Washio, A. & Kitamura, C. Current and future options for dental pulp therapy. *Jpn Dent. Sci. Rev.* **55**, 5–11 (2019).
5. Chen, J., Xu, H., Xia, K., Cheng, S. & Zhang, Q. Resolvin E1 accelerates pulp repair by regulating inflammation and stimulating dentin regeneration in dental pulp stem cells. *Stem Cell. Res. Ther.* **12**, 75 (2021).
6. Cooper, P. R., Holder, M. J. & Smith, A. J. Inflammation and regeneration in the Dentin-Pulp complex: A Double-Edged sword. *J. Endod.* **40**, S46–S51 (2014).
7. Hui, T. et al. Ezh2, a potential regulator of dental pulp inflammation and regeneration. *J. Endod.* **40**, 1132–1138 (2014).
8. Li, Y., Han, J., Wang, Y. & Lei, S. Effects of Epigallocatechin gallate (Egcg) on the biological properties of human dental pulp stem cells and inflammatory pulp tissue. *Arch. Oral Biol.* **123**, 105034 (2021).
9. Arora, S. et al. Potential application of immunotherapy for modulation of pulp inflammation: opportunities for vital pulp treatment. *Int. Endod J.* **54**, 1263–1274 (2021).
10. Johnson, J. J. & Carnosol A promising Anti-Cancer and Anti-Inflammatory agent. *Cancer Lett.* **305**, 1–7 (2011).
11. Brieskorn, C. H. Fuchs A;Brendenberg JB;McChesney JD & E, W. The structure of carnosol. *J. Org. Chem.* **29**, 2293–2298 (1964).
12. Kashyap, D. et al. Mechanistic insight into Carnosol-Mediated Pharmacological effects: recent trends and advancements. *Life Sci.* **169**, 27–36 (2017).
13. Yeo, I. J. et al. Inhibitory effect of carnosol on Uvb-Induced inflammation via Inhibition of Stat3. *Arch. Pharm. Res.* **42**, 274–283 (2019).
14. Li, L., Pan, Z., Ning, D. & Fu, Y. Rosmanol and Carnosol Synergistically Alleviate Rheumatoid Arthritis through Inhibiting Tlr4/Nf-Kb/Mapk Pathway. *Molecules.* 27. (2021).
15. Li, X. et al. Carnosol modulates Th17 cell differentiation and microglial switch in experimental autoimmune encephalomyelitis. *Front. Immunol.* **9**, 1807 (2018).
16. de Oliveira, J. R. et al. Biological activities of *Rosmarinus officinalis* L. (Rosemary) extract as analyzed in microorganisms and cells. *Exp. Biol. Med.* **242**, 625–634 (2017).
17. Monsen, R. E. et al. A mouth rinse based on a tea solution of salvia officinalis for oral discomfort in palliative cancer care: A randomized controlled trial. *Support Care Cancer.* **29**, 4997–5007 (2021).
18. Taheri, J. B., Azimi, S., Rafieian, N. & Zanjani, H. A. Herbs in dentistry. *Int. Dent. J.* **61**, 287–296 (2011).
19. ESCOP. *Monographs on the Medicinal Uses of Plant Drugs* (European Scientific Cooperative on Phytotherapy, 1996).
20. Mendes, F. et al. Antibacterial activity of *salvia officinalis* L. Against periodontopathogens: an in vitro study. *Anaerobe* **63**, 102194 (2020).
21. Rodrigues, M. R. et al. Antinociceptive and Anti-Inflammatory potential of extract and isolated compounds from the leaves of salvia officinalis in mice. *J. Ethnopharmacol.* **139**, 519–526 (2012).
22. Valones, M. et al. Clinical assessment of Rosemary-Based toothpaste (Rosmarinus officinalis Linn.): A randomized controlled Double-Blind study. *Braz Dent. J.* **30**, 146–151 (2019).
23. Dong, H., Zhang, Y., Huang, Y. & Deng, H. Pathophysiology of Rage in inflammatory diseases. *Front. Immunol.* **13**, 931473 (2022).

24. Reynolds, P. R., Wasley, K. M. & Allison, C. H. Diesel particulate matter induces receptor for advanced glycation End-Products (Rage) expression in pulmonary epithelial Cells, and Rage signaling influences Nf-Kb-Mediated inflammation. *Environ. Health Perspect.* **119**, 332–336 (2011).
25. Hudson, B. I. & Lippman, M. E. Targeting Rage signaling in inflammatory disease. *Annu. Rev. Med.* **69**, 349–364 (2018).
26. Ramasamy, R., Shekhtman, A. & Schmidt, A. M. The Rage/Diaph1 signaling axis & implications for the pathogenesis of diabetic complications. *Int J. Mol. Sci* 23. (2022).
27. Schmidt, A. M. Diabetes mellitus and cardiovascular disease. *Arterioscler. Thromb. Vasc Biol.* **39**, 558–568 (2019).
28. Reddy, V. P., Aryal, P. & Soni, P. Rage Inhibitors in Neurodegenerative Diseases. *Biomedicines*. 11. (2023).
29. Sims, G. P., Rowe, D. C., Rietdijk, S. T., Herbst, R. & Coyle, A. J. Hmgb1 and Rage in inflammation and cancer. *Annu. Rev. Immunol.* **28**, 367–388 (2010).
30. Ding, B. et al. Tanshinone Iia attenuates neuroinflammation via inhibiting Rage/Nf-Kb signaling pathway in vivo and in vitro. *J. Neuroinflamm*. **17**, 302 (2020).
31. Tancharoen, S. et al. Overexpression of Receptor for Advanced Glycation End Products and High-Mobility Group Box 1 in Human Dental Pulp Inflammation. *Mediat. Inflamm.* 2014, 754069. (2014).
32. Zhang, X. et al. Expression of high mobility group box 1 in inflamed dental pulp and its chemotactic effect on dental pulp cells. *Biochem. Biophys. Res. Commun.* **450**, 1547–1552 (2014).
33. Abdul, G. M., Ugusman, A., Latip, J. & Zainalabidin, S. Role of terpenophenolics in modulating inflammation and apoptosis in cardiovascular diseases: A review. *Int J. Mol. Sci* 24. (2023).
34. Avila-Carrasco, L. et al. Natural plants compounds as modulators of Epithelial-to-Mesenchymal transition. *Front. Pharmacol.* **10**, 715 (2019).
35. Bernardes, W. A. et al. Antimicrobial activity of Rosmarinus officinalis against oral pathogens: relevance of carnosic acid and carnosol. *Chem. Biodivers.* **7**, 1835–1840 (2010).
36. Chen, Y. et al. Carnosol attenuates Rankl-Induced osteoclastogenesis in vitro and Lps-Induced bone loss. *Int. Immunopharmacol.* **89**, 106978 (2020).
37. Schwager, J., Richard, N., Fowler, A., Seifert, N. & Raederstorff, D. Carnosol and related substances modulate chemokine and cytokine production in macrophages and chondrocytes. *Molecules* **21**, 465 (2016).
38. Yao, H. et al. Carnosol inhibits cell adhesion molecules and chemokine expression by tumor necrosis Factor-A in human umbilical vein endothelial cells through the nuclear Factor-Kb and Mitogen-Activated protein kinase pathways. *Mol. Med. Rep.* **9**, 476–480 (2014).
39. Yao, J. H. et al. Prophylaxis with carnosol attenuates liver injury induced by intestinal Ischemia/Reperfusion. *World J. Gastroenterol.* **15**, 3240–3245 (2009).
40. Yan, Y., Liu, Y., Yang, Y., Ding, Y. & Sun, X. Carnosol suppresses microglia cell inflammation and apoptosis through Pi3K/Akt/Mtor signaling pathway. *Immunopharmacol. Immunotoxicol.* **44**, 656–662 (2022).
41. Shi, W. et al. Carnosol inhibits inflammasome activation by directly targeting Hsp90 to treat inflammasome-Mediated diseases. *Cell. Death Dis.* **11**, 252 (2020).
42. Monu et al. Transthyretin and receptor for advanced glycation end product's differential levels associated with the pathogenesis of rheumatoid arthritis. *J. Inflamm. Res.* **14**, 5581–5596 (2021).
43. Arab, H. H., Al-Shorbagy, M. Y. & Saad, M. A. Activation of autophagy and suppression of apoptosis by Dapagliflozin attenuates experimental inflammatory bowel disease in rats: targeting Ampk/Mtor, Hmgb1/Rage and Nrf2/Ho-1 pathways. *Chem. -Biol Interact.* **335**, 109368 (2021).
44. Manigrasso, M. B., Juranek, J., Ramasamy, R. & Schmidt, A. M. Unlocking the biology of Rage in diabetic microvascular complications. *Trends Endocrinol. Metab.* **25**, 15–22 (2014).
45. Sathe, K. et al. S100B is increased in parkinson's disease and ablation protects against Mptp-Induced toxicity through the Rage and Tnf-A pathway. *Brain* **135**, 3336–3347 (2012).
46. Body-Malapel, M. et al. The Rage signaling pathway is involved in intestinal inflammation and represents a promising therapeutic target for inflammatory bowel diseases. *Mucosal Immunol.* **12**, 468–478 (2019).
47. Manigrasso, M. B. et al. Small-Molecule antagonism of the interaction of the Rage cytoplasmic domain with Diaph1 reduces diabetic complications in mice. *Sci. Transl Med.* **13**, eabf7084 (2021).
48. Monu;Agnihotri, P., Saquib, M. & Biswas, S. Targeting Tnf-A-Induced Expression of Ttr and Rage in Rheumatoid Arthritis: Apigenin's Mediated Therapeutic Approach. *Cytokine*. 179, 156616. (2024).
49. Liu, Y., Beyer, A. & Aebersold, R. On the dependency of cellular protein levels on Mrna abundance. *Cell* **165**, 535–550 (2016).
50. Tang, Y., Wang, J., Cai, W. & Xu, J. Rage/Nf-Kb pathway mediates Hypoxia-Induced insulin resistance in 3T3-L1 adipocytes. *Biochem. Biophys. Res. Commun.* **521**, 77–83 (2020).

Acknowledgements

We would like to thank the patients for their contributions to this study.

Author contributions

Xinpai Liu and Chunhui Zhao: conceptualisation, methodology, formal analysis, and writing—original draft preparation. Xirun Zong and Wenjing Fang: data curation, formal analysis, and validation. Jing Zhang, Wei He, and Wuli Li: conceptualisation, methodology, supervision, review, and editing. The final version of the manuscript was reviewed, edited, and approved by all authors.

Funding

This work was supported by the Disciplinary Construction Project in the School of Dentistry of Anhui Medical University [grant numbers 2022xkfyts05 and 2023xkfyhz04] and the Scientific Research Funding of Anhui Province Health Commission [grant number AHWJ2023A20112].

Declarations

Competing interests

The authors declare no competing interests.

Institutional review board statement

The study was conducted in accordance with the Declaration of Helsinki, and approved by the Ethics Committee of the Affiliated Stomatology Hospital of Anhui Medical University (approval no. T2022023).

The animal study protocol was approved by the Ethics Committee of Anhui Medical University (approval no. LLSC20221248).

Informed consent

Informed consent was obtained from all subjects involved in the study.

Additional information

Supplementary Information The online version contains supplementary material available at https://doi.org/10.1038/s41598-025-28542-0.

Correspondence and requests for materials should be addressed to J.Z., W.H. or W.L.

Reprints and permissions information is available at www.nature.com/reprints.

Publisher's note Springer Nature remains neutral with regard to jurisdictional claims in published maps and institutional affiliations.